# Oblique Wing Aircraft Flight Control System

R. N. Clark*
*University of Washington, Seattle, Washington*
and
X. J. Y. LeTron†
*Aerospatiale of France, Toulouse, France*

**A design procedure for a command and stability augmentation system (CSAS) for the oblique wing research airplane (OWRA) is presented. Three flight conditions are considered in which the wing skew angle is 0, 55, and 65 deg. The wing skew angle in the latter two cases induces severe asymmetrical dynamic behavior of the airframe. Five primary flight control surfaces are used to decouple the longitudinal motions from the lateral motions. The CSAS must accept conventional three-axis stick and rudder inputs from the pilot and translate these, along with feedback signals from the airframe, into the five airframe control surface commands. The design procedure combines eigenstructure design principles with an optimization scheme, providing a closed-loop response to both pilot inputs and to initial conditions that approximate those obtained with the wing in the unskewed position. The control surface deflections and rates required are within the capability of the OWRA for small-amplitude maneuvers.**

## Introduction

OBLIQUE wing aircraft (OWA) offer attractive potential advantages over straight wing aircraft due to superior lift to drag ratios in supersonic, and even subsonic, flight.[1] However, the asymmetry of OWA can introduce flight control problems that are not present in conventional aircraft.[2,3] This paper considers the primary flight control system of the NASA oblique wing research aircraft (OWRA).[4] This aircraft has a wing skew angle that is variable from 0 to 65 deg, and has five primary flight control surfaces: left stabilizer, right stabilizer, left aileron, right aileron, and rudder. The pronounced asymmetry of the OWRA, especially at large wing skew angles, indicates that these five surfaces should be controlled independently from one another, so that the primary flight control input to the airframe has five independent components as compared to the three primary inputs that are sufficient in a symmetrical aircraft.

Acceptable handling qualities for the OWRA may require that the pilot-airplane interface be the conventional three-axis "stick and rudder." The decoupling of the longitudinal motions of the asymmetrical airframe from the lateral motions will be accomplished by a command and stability augmentation system (CSAS). This CSAS accepts the three conventional pilot inputs, mixes these appropriately with feedback signals from the airframe, and generates the five independent control surface commands required to decouple the longitudinal and lateral motions.

This CSAS design problem is approached here by first establishing a set of desired response characteristics to the conventional pilot inputs. These desired characteristics are taken simply to be the response of the airframe in a given flight condition for which the wing skew angle is zero. In this flight condition the aircraft is nearly symmetrical and the coupling between the longitudinal and lateral motions is negligible insofar as gross handling quality is concerned. Multivariable control theory is then applied to establish a desired eigenstructure for the CSAS-airframe combination, assuming that the CSAS itself uses no dynamic compensation.[5-7] Eigenstructure assignment techniques are combined with an optimization procedure to determine the feedback matrix that provides an eigenstructure that approximates the desired eigenstructure for a flight condition in which the wing skew angle is large. In this way the zero input response (ZIR) of the skewed wing aircraft is made to approximate the desired zero input response. A feed-forward matrix is also necessary to translate the three conventional pilot inputs into the five independent airframe control surface inputs.

## Airframe and Actuator Models

Reference 4 provides dynamic models of the airframe, actuators, and sensors for the OWRA. There are six such models in Ref. 4, one for each of six different flight conditions of level, trimmed flight at six different combinations of altitude, Mach number, and wing skew angle. We refer to only three of these flight conditions here, designated as FC1, FC3, and FC6 (following the notation of Ref. 4) as noted in Table 1. Each of the given models is a linear, constant coefficient, matrix differential equation of order 10. These models represent the dynamics of the airframe when driven by small displacements of the five primary control surfaces from their equilibrium positions for trimmed straight and level flight.

The state vector of the airframe is

$$x_{AF} = \begin{bmatrix} x_1 \\ x_2 \\ x_3 \\ x_4 \\ x_5 \\ x_6 \\ x_7 \\ x_8 \\ x_9 \\ x_{10} \end{bmatrix} = \begin{bmatrix} v \text{ ft/s} \\ h \text{ feet} \\ \alpha \text{ radians} \\ \beta \text{ radians} \\ \phi \text{ radians} \\ \theta \text{ radians} \\ \psi \text{ radians} \\ p = \dot{\phi} \text{ rad/s} \\ q = \dot{\theta} \text{ rad/s} \\ r = \dot{\psi} \text{ rad/s} \end{bmatrix} \tag{1}$$

The control vector of the airframe is

$$u_{AF} = \begin{cases} \delta_{eL}, \text{ left stabilizer deflection, radians} \\ \Delta_{eR}, \text{ right stabilizer deflection, radians} \\ \delta_{AL}, \text{ left aileron deflection, radians} \\ \delta_{AR}, \text{ right aileron deflection, radians} \\ \delta_{R}, \text{ rudder deflection, radians} \end{cases} \tag{2}$$

Received April 10, 1987; revision received Sept. 10, 1987. 

*Professor of Electrical Engineering, Professor of Aeronautics and Astronautics. Associate Fellow AIAA.
†Engineer of Aerospatiale, A/DET/EG/QDV.

**Table 1 Flight conditions for OWRA[a]**

| F.C. | Altitude, ft | Mach number | Wing skew angle, deg[b] | Dynamic pressure, lb/ft$^2$ |
|---|---|---|---|---|
| 1 | 15,000 | 0.6 | 0 | 301 |
| 3 | 20,000 | 0.9 | 55 | 552 |
| 6 | 30,000 | 1.4 | 65 | 540 |

[a]From Ref. 4. [b]Right wing forward.

**Table 2 Actuator characteristics**

| Actuator | Deflection limit, deg | Rate limit, deg/s | Time constant, s |
|---|---|---|---|
| Stabilizers | +6<br>−24.5 | ±25 | 0.0667 |
| Ailerons | ±30 | ±50 | 0.050 |
| Rudder | ±10 | ±60 | 0.025 |

where $\delta_{eL}, \delta_{eR}, \delta_{AL}, \delta_{AR} > 0$ means the trailing edge is displaced downward, and $\delta_R > 0$ means the trailing edge is displaced to the left.

The dynamic equation for the airframe, in standard state-variable form, is

$$\dot{x}_{AF} = A_{AF} x_{AF} + B_{AF} u_{AF} \tag{3}$$

The elements of the $A_{AF}$ and $B_{AF}$ matrices for flight conditions 1, 3, and 6 are given in Ref. 4 and are also listed here in Appendix A.

The five actuator servomechanisms are characterized by the data in Table 2. Each is assumed here to behave as a first-order linear system with the time constants noted. The deflection and rate limits noted in the table are not invoked in the present analysis, which is only valid for deflections and rates less than those indicated. Thus, the state-variable model for the actuator servomechanisms is

$$\dot{x}_{\text{act}} = A_{\text{act}} x_{\text{act}} + B_{\text{act}} u \tag{4}$$

where

$$x_{\text{act}} = u_{AF} \tag{5}$$

[see Eq. (2)]

$$u = \begin{bmatrix} \delta_{eLC} \\ \delta_{eRC} \\ \delta_{ALC} \\ \delta_{ARC} \\ \delta_{RC} \end{bmatrix} = \begin{bmatrix} \text{the commanded} \\ \text{control surface} \\ \text{deflections} \end{bmatrix} \tag{6}$$

$$A_{\text{act}} = \begin{bmatrix} -15 & 0 & 0 & 0 & 0 \\ 0 & -15 & 0 & 0 & 0 \\ 0 & 0 & -20 & 0 & 0 \\ 0 & 0 & 0 & -20 & 0 \\ 0 & 0 & 0 & 0 & -40 \end{bmatrix} \tag{7}$$

$$B_{\text{act}} = -A_{\text{act}} \tag{8}$$

We consider the actuator-airframe combination as a single fifteenth-order system having $u$ as the input vector and $x$ as the state vector, where

$$x = \begin{bmatrix} x_{\text{AF}} \\ x_{\text{act}} \end{bmatrix} \tag{9}$$

**Table 3 Ten eigenvalues of $A_1$ corresponding to the airframe motion (flight condition 1, $\Delta = 0$)**

| Longitudinal modes (five) | | Lateral modes (five) | |
|---|---|---|---|
| $-0.84 \pm j2.49$ | (short period) | 0 | (heading) |
| $-0.0025 \pm j0.0698$ | (phugoid) | −0.0134 | (spiral) |
| −0.0012 | (convergent) | −5.94 | (roll convergence) |
| | | $-0.41 \pm j2.59$ | (dutch roll) |

Thus, the state-variable model for this combined system is

$$\dot{x} = Ax + Bu \tag{10}$$

where

$$A = \begin{bmatrix} A_{AF} & B_{AF} \\ 0 & A_{\text{act}} \end{bmatrix}, \quad B = \begin{bmatrix} 0 \\ B_{\text{act}} \end{bmatrix} \tag{11}$$

There are 13 sensors providing air data and inertial measurements on the OWRA. The five actuators also have position sensors so that the output signal vector in this case is $y$:

$$y = C_o x \tag{12}$$

where $C_o$ is an 18 × 15 matrix of full rank. Most of the state variables are measured directly in the output vector $y$, and because $C_0$ is full rank, it is reasonable to assume that the full state vector $x$ is available for feedback to the CSAS; $x$ is the 15th-order state defined by Eqs. (1), (2), (5), and (9).

We adopt the notation that the $A$ matrix in Eq. (10) will be denoted as $A_1$ for FC1, $A_3$ for FC3, and $A_6$ for FC6. Similarly, the state vectors and input vectors for the three flight conditions will be denoted by superscripts $x^1(t)$ and $u^1(t)$, $x^3(t)$ and $u^3(t)$, and $x^6(t)$ and $u^6(t)$. The $B$ matrix is the same for all three flight conditions, as is evident from Eq. (11). It is also evident from Eq. (11) that $A_1$, $A_3$, and $A_6$ are composed of the elements $a_{ij}$ and $b_{ij}$ of the $A_{AF}$ and $B_{AF}$ matrices for the corresponding flight conditions given in Appendix A, along with the $A_{\text{act}}$ matrix, which is the same for all three flight conditions, given in Eq. (7). The eigenvalues of $A$ are obviously the five fixed eigenvalues of $A_{\text{act}}$ along with the 10 eigenvalues of $A_{AF}$, which are different for each flight condition. However, in each of the three subject flight conditions, all 15 eigenvalues lie in the left-half plane, and the 15th-order actuator-airframe combination is fully state controllable through the input vector $u(t)$.

The coupling from the longitudinal motion of the airframe into the lateral motion is evident from the coefficients of the $A$ matrix given in Appendix A. For example, $a_{89}$ indicates the roll moment that is induced by pitch rate, and $a_{8,10}$ indicates the roll moment induced by yaw rate. Both of these coefficients are significantly larger in FC3 and FC6 than in FC1. Similarly, coupling from the lateral motion into the longitudinal motion is evident from coefficients $a_{98}$ and $a_{9,10}$ again with predominance of those coefficients in FC3 and FC6 over those in FC1. This coupling is illustrated in Fig. 1, which shows the pitch, roll, and yaw motions of the airframe for a ZIR. This means the control input vector is held fixed at zero (no control surface deflections occur), whereas the initial state vector $x_0$ has all zero elements except for $\dot{\theta}(0) = x_9(0)$, which is taken to be 1 deg/s.

The coupling is minimal in FC1 and is probably due to the gyroscopic effect of the rotating mass of the engine. The coupling is pronounced in FC3 and in FC6, due, of course, to the asymmetry of the airframe with the wing in the skewed position. Only the first 10 s of the ZIR is shown here, as this shows the short period motion.

We take the response shown in Fig. 1 for FC1 as the design criterion for the desired ZIR in this work. This ZIR is

$$x^1(t) = \epsilon^{A_1 t} x_0 \tag{13}$$

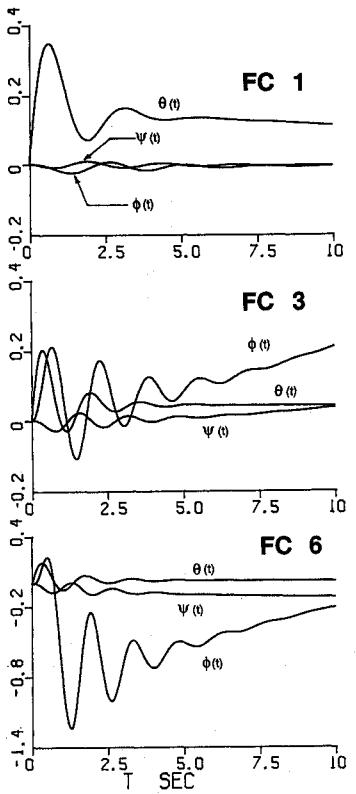


**Fig. 1 Zero input response to $\dot{\theta}_o = 1$ deg/s for the three subject flight conditions. Deflections given in degrees.**

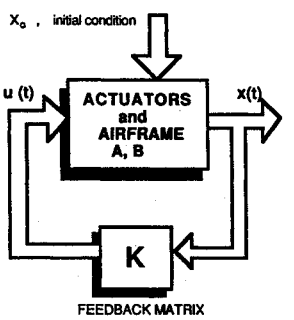


**Fig. 2 Block diagram of system for control law design for ZIR.**

where $\epsilon^{A_1 t}$ is the 15 × 15 "state transition matrix," and $x_0$ is the initial state vector:

$$x_0 = [00\cdots010\cdots0]^T \tag{14}$$

where the 1 appears as the 9th element [$\dot{\theta}(0) = 1$ deg/s]. Of course, only three of the 15 state variables from $x^1(t)$ are shown in Fig. 2: $x_5^1(t)$, $x_6^1(t)$, and $x_7^1(t)$. It is well known that the response $x^1(t)$ given in Eq. (13) may also be written as

$$x^1(t) = V_1\epsilon^{\lambda_1 t} + V_2\epsilon^{\lambda_2 t} + \cdots + V_{15}\epsilon^{\lambda_{15} t} \tag{15}$$

where $\lambda_1, \lambda_2, \ldots \lambda_{15}$ are the eigenvalues of $A_1$, which are distinct, and $V_i$ is an eigenvector of $A_1$ corresponding to eigenvalue $\lambda_i$. The eigenvectors are constrained by the given initial state vector to satisfy

$$x_0 = \sum_{i=1}^{15} V_i \tag{16}$$

**Table 4 Eigenvectors of $A_1$ for ZIR of Eq. (15) listed with corresponding eigenvalue[a]**

| −5.94 | −0.84 + j2.49 | −0.41 + j2.59 |
|---|---|---|
| 0.1403 | −38.96 + j48.63 | −44.05 + j42.43 |
| 1.7771 | −307.3 − j949 | −77.07 − j881.4 |
| 0.1051 | −3.418 + j10.47 | −1.938 + j9.475 |
| 3.787 | −0.03139 − j1.078 | 24.96 − j85.13 |
| −166.0 | 1.272 − j1.217 | 132.5 − j30.28 |
| 0.08851 | 0.7213 + j10.53 | 1.714 + j9.733 |
| −3.271 | 0.1018 + j1.03 | −17.28 + j84.28 |
| 985.9 | 1.979 + j4.204 | 25.58 + j356.5 |
| −0.5257 | −26.85 − j7.104 | −25.94 + j0.429 |
| 19.43 | −2.655 − j.6175 | −211.4 − j79.55 |
| 0 | 0 | 0 |
| 0 | 0 | 0 |
| 0 | 0 | 0 |
| 0 | 0 | 0 |
| 0 | 0 | 0 |

| −0.0025 + j0.0698 | −0.0012 | −0.0134 | 0 |
|---|---|---|---|
| −50.42 + j3.322 | 12.67 | −80.1 | 0 |
| 985.2 − j163.9 | 1000. | 994.8 | 0 |
| 0.003146 − j0.000165 | −0.00069 | 0.01655 | 0 |
| −0.000098 − j0.00002 | 0 | 0.08205 | 0 |
| 0.00011 − j0.006525 | −0.000015 | 16.33 | 0 |
| 0.01725 + j0.1089 | −0.00259 | −0.004459 | 0 |
| −0.004616 − j0.000266 | 0.000642 | −60.78 | 1000.0 |
| 0.000455 + j0.000027 | 0 | −0.2255 | 0 |
| −0.00765 + j0.000928 | 0.000003 | 0.00006 | 0 |
| 0.00003 − j0.00032 | 0 | 0.8144 | 0 |
| 0 | 0 | 0 | 0 |
| 0 | 0 | 0 | 0 |
| 0 | 0 | 0 | 0 |
| 0 | 0 | 0 | 0 |
| 0 | 0 | 0 | 0 |

| −15 | −15 | −20 | −20 | −40 |
|---|---|---|---|---|
| −103.2 | −103 | 21.46 | 21.47 | 0.00209 |
| 135.2 | 135.2 | 40.40 | 40.42 | 0.001582 |
| −17.6 | −17.51 | 1.06 | 1.078 | 0.00668 |
| −2.994 | 3.25 | −1 | 1.002 | 1.346 |
| 40.93 | −41.04 | 40.18 | −40.18 | 4.383 |
| −20.80 | −20.7 | −0.2137 | −0.196 | 0.00658 |
| 3.653 | −3.906 | 1.144 | −1.146 | −2.658 |
| −613.5 | 615.1 | −803.4 | 803.4 | −176.2 |
| 311.9 | 310.5 | 4.275 | 3.919 | −0.2632 |
| −54.8 | 58.59 | −22.88 | 22.92 | 106.3 |
| 701.4 | 0 | 0 | 0 | 0 |
| 0 | 700.3 | 0 | 0 | 0 |
| 0 | 0 | 591.8 | 0 | 0 |
| 0 | 0 | 0 | 591.8 | 0 |
| 0 | 0 | 0 | 0 | 978.6 |

[a]Complex conjugate eigenvectors and eigenvalues are not listed.

The fifteen eigenvalues of $A_1$ along with their corresponding eigenvectors are called the eigenstructure of the desired response $x^1(t)$.

The 10 eigenvalues of $A_1$ pertaining to the airframe motion in FC1 are listed in Table 3. The five eigenvalues pertaining to the five actuators are the numbers on the diagonal of $A_{act}$ [Eq. (7)]. A set of eigenvectors of $A_1$, each corresponding to one of the 15 eigenvalues, is listed in Table 4. Note that the last five elements of each eigenvector is zero because the five state variables $\delta_{eL}$, $\delta_{eR}$, $\delta_{AL}$, $\delta_{AR}$, and $\delta_R$ all remain zero during this ZIR manuever. The identity of the modes listed in Table 3 comes from the magnitudes of the eigenvector components listed in Table 4. The spiral mode, for example, is identified as having the eigenvalue −0.0134 because the three predominant numbers in that column in Table 4 correspond to $x_2$, the altitude, $x_1$, the airspeed, and $x_7$, the heading. The coefficient corresponding to $x_5$, the roll angle, is also significant. The pitch

convergence mode (eigenvalue $-0.0012$) is similarly identified because only those coefficients corresponding to $x_1$ and $x_2$ have significant magnitudes.

We seek a CSAS design for FC3 and FC6 that will provide an airframe response resembling that achieved in FC1, illustrated in Fig. 1. We also require as part of the design performance criterion that the control surface deflections demanded by the CSAS during this ZIR manuever be within the limits prescribed in Table 2 when the initial conditions are small.

## Feedback Matrix Design

Figure 2 shows the first step in the CSAS design. With the $5 \times 15$ "control law" matrix $K$ providing feedback from all 15 state variables to all 5 actuator inputs, we have

$$u = Kx \tag{17}$$

Combined with Eq. (10) this gives the closed-loop dynamic equation

$$\begin{aligned} \dot{x} &= [A + BK]x \\ x(0) &= x_0 \end{aligned} \tag{18}$$

where $x_0$ is given in Eq. (14). To maintain consistent notation the matrix in Eq. (18) is, for FC3, $[A_3 + BK_3]$ and, for FC6, it is $[A_6 + BK_6]$. We wish to find the feedback matrix $K_3$ (for FC3) such that the eigenstructure of $[A_3 + BK_3]$ resembles that of $A_1$, insofar as the airframe motion is concerned. We carefully note that we do not want to match the last five elements of the eigenvectors of $[A_3 + BK_3]$ to those given for $A_1$ in Table 4. If such a matrix $K_3$ can be found, the ZIR for FC3, which is

$$x^3(t) = \epsilon^{[A_3 + BK_3]t} x_0 \tag{19}$$

will closely resemble $x^1(t)$ given in Eq. (13) in its first 10 state variables—those pertaining to the airframe motion. The last five state-variable fluctuations are the control surface deflections produced by the feedback connection, which are required to make the asymmetrical airframe (FC3) behave like the symmetrical airframe (FC1).

We identify the 10 eigenvalues of $A_1$ that pertain to the airframe motion, and the 10 corresponding engenvectors as $\lambda_{id}$ and $V_{id}$ for $i = 1,2,...10$. These are the desired eigenvalues and eigenvectors for $[A_3 + BK_3]$ and $[A_6 + BK_6]$. We use a composite design criterion for the choice of $K_3$ in FC3 that minimizes the differences $(\gamma_i^3 - \lambda_{id})$ and $(V_i^3 - V_{id})$, where $\gamma_i^3$ and $V_i^3$ are the eigenstructure of $[A_3 + BK_3]$. The design criterion for FC6 is similar.

We proceed now with the determination of $K_3$ for FC3. Following Wonham,[8] we note that $\gamma_i$ and $V_i^3$ $(i = 1,2,...15)$ are eigenvalues and eigenvectors of $[A_3 + BK_3]$ if and only if there exists a vector $w_i$, such that

$$[A_3 - \gamma_i I]V_i^3 + Bw_i = 0 \tag{20}$$

where $w_i = K_3 V_i^3$. The design problem is formulated as follows. A feedback matrix $K_3$ is to be found such that the criterion $C_i$

$$C_i = \alpha_i|\gamma_i - \lambda_{id}|^2 + \|V_i^3 - V_{id}\|_{Q_i}^2 + \beta_i\|w_i\|^2 \tag{21}$$

is minimized, subject to the constraint in Eq. (20). Here $i = 1,2,...15$, omitting one number for each pair of complex eigenvalues, and $\alpha_i$ and $\beta_i$ are real, positive, weighting coefficients. The notation $\|V\|_{Q_i}^2$ means

$$\|V\|_{Q_i}^2 = V^T Q_i \bar{V} \tag{22}$$

where $Q_i$ is diagonal and positive definite:

$$Q_i = \text{diag}\{q_{ii}\} \tag{23}$$

A descent method for finding the minimum $C_i$ is described in detail in Appendix B. The result of this minimizing operation is the set of 15 eigenvalues $\{\gamma_i\}$, 15 eigenvectors $\{V_i^3\}$, and 15 vectors $\{w_i\}$. From these we form

$$w = [w_i\ w_2 \cdots w_{15}] = K_3[V_1^3\ V_2^3 \cdots V_{15}^3] \tag{24}$$

from which the feedback matrix $K_3$ is given by

$$K_3 = w[V_1^3 V_2^3 \cdots V_{15}^3]^{-1} \tag{25}$$

This $K_3$ matrix is then tested by simulating the initial value problem

$$\dot{x} = [A_3 + BK_3]x \tag{26a}$$

$$x_0[00\cdots1\cdots0]^T \tag{26b}$$

where $x_0$ is given by Eq. (14). The solution to Eq. (26), $x^3(t)$, was compared to the corresponding solution for FC1. Excessive motion in the lateral axes was observed. To correct this the eigenstructure of $[A_3 + BK_3]$ was compared to that of $A_1$ to determine which elements of which eigenvectors were responsible for the undesired coupling. These elements were corrected by repeating the optimization procedure with changes in the coefficients $\alpha_i$ and $q_{ii}$ to place more weight on these identified elements. This resulted in a new $K_3$, which was also tested in a similar way. This re-optimization process had to be repeated two or three times until a $K_3$ resulted that provided a satisfactory ZIR for the $\dot{\theta}_0 = 1$ deg/s case.

The simulation was then tested for a ZIR in which the initial state vector was $x_0 = [00\cdots010\cdots0]^T$ where the 1 was $\dot{\phi}_0 = x_8(0) = 1$ deg/s. This test showed a ZIR quite similar to that obtained in a corresponding test for FC1. Then a similar test for $\alpha_0 = x_3(0) = 1$ deg was conducted, but the ZIR obtained in FC3 did not match that obtained in a corresponding test for FC1 to a satisfactory degree. This occasioned another two or three iterations of the optimization procedure as described above. A new $K_3$ matrix was obtained and this proved to give responses in FC3 that satisfactorily matched all three of the ZIR tests ($\dot{\theta}_0$, $\dot{\phi}_0$, and $\alpha_0$) obtained in FC1.

For the FC6 a similar scenario was followed. By starting the optimization procedure with the 17 weighting coefficients $\alpha_i$, $\beta_i$, $q_{ii}$, which were the final ones found for FC3, the first $K_6$ matrix found for FC6 gave better results in the initial condition tests than was the case in FC3 (where the first trial set of 17 weighting coefficients were chosen arbitrarily). Nevertheless, some reiteration of the optimization procedure was also necessary in FC6.

The $K_3$ and $K_6$ matrices that we found to produce satisfactory performance in the initial condition tests required further refinement to satisfy the requirements for the pilot input commands. This is described in the following section.

## Feed-Forward Matrix Design

The pilot inputs are assumed to be three conventional commanded control surface deflections. These are coupled into the system through a $(5 \times 3)$ matrix $L$, as shown in Fig. 3. Here

$$u_p = [\delta_{eC}\delta_{AC}\delta_{RC}]^T \tag{27}$$

For FC1, $L_1$ is taken to be

$$L_1 = \begin{bmatrix} 1 & 0 & 0 \\ 1 & 0 & 0 \\ 0 & 1 & 0 \\ 0 & -1 & 0 \\ 0 & 0 & 1 \end{bmatrix} \tag{28}$$

so that the stabilizer and aileron commands are symmetrical, as is the case for a conventional airplane.

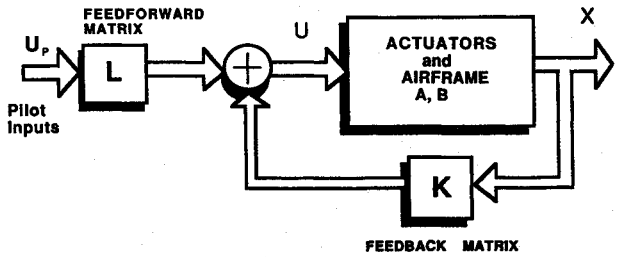


**Fig. 3 Coupling pilot inputs to feedback signals.**

**Table 5 $L$ matrix elements**

| Elements | FC1 | FC3 | FC6 |
|---|---|---|---|
| $l_{11}$ | 1 | 0.286 | 2.62 |
| $l_{12}$ | 0 | 0.027 | 0.442 |
| $l_{13}$ | 0 | −0.452 | 0.485 |
| $l_{21}$ | 1 | 0.566 | 1.306 |
| $l_{22}$ | 0 | −0.260 | −0.393 |
| $l_{23}$ | 0 | 0.312 | 0.0365 |
| $l_{31}$ | 0 | 1.82 | −0.976 |
| $l_{32}$ | 1 | 1.79 | 0.32 |
| $l_{33}$ | 0 | 1.305 | −11.5 |
| $l_{41}$ | 0 | 0.51 | 8.46 |
| $l_{42}$ | −1 | −0.41 | −0.272 |
| $l_{43}$ | 0 | −0.0291 | −0.846 |
| $l_{51}$ | 0 | −0.026 | −0.126 |
| $l_{52}$ | 0 | 0.033 | 0.097 |
| $l_{53}$ | 1 | −0.07 | 1.3 |

Now the relationship between the pilot's inputs $u_p$ and the airplane-CSAS combination is

$$\dot{x} = [A + BK]x + [BL]u_p \tag{29}$$

where for FC1, $A = A_1$, $L = L_1$, and $K = 0$. For FC3, $A = A_3$, $L = L_3$, and $K = K_3$, and similarly for FC6.

To establish a performance criterion for the airframe in response to the pilot's stabilizer command $\delta_{eC}(t)$, a step command of 1 deg, lasting for 2 s, is applied with the aircraft in FC1. That is,

$$\delta_{eC}(t) = S(t) - S(t-2) \tag{30}$$

where $S(t)$ is the unit step function. The response of the airframe state variables, principally $\alpha$, $\beta$, $\dot{\phi}$, $\dot{\psi}$, and $\dot{\theta}$ were taken to be the desired responses to this input pulse. Similar sets of responses for 1 deg pulse inputs on $\delta_{AC}$ and $\delta_{RC}$ were also established.

Considering FC3, we must find an $L_3$ such that the solution to Eq. (29), with the standard 2-s pulse of $\delta_{eC}(t)$, will approximate that found in FC1, and with reasonable control surface deflections (that are now governed by the feedback commands as well as the pilot commands). To achieve this we attempted to choose $L_3$ so that the initial values of $\ddot{\alpha}$, $\ddot{\beta}$, $\ddot{\phi}$, $\ddot{\psi}$, and $\ddot{\theta}$, namely $\ddot{\alpha}(0^+)$, $\ddot{\beta}(0^+)$, etc. in FC3, matched the corresponding initial values realized in the standard tests in FC1. This matching yields a unique solution for $L_3$. However, this $L_3$, along with the $K_3$ found for the ZIR case to reduce cross-axis coupling, proved to cause excessive control surface movements in response to the pilot's stabilizer command pulse. This was corrected by re-entering the optimization process, as described above, and increasing the weighting coefficients $q_{ii}$ corresponding to the actuator states. Several iterations of this procedure yielded another new $K_3$ which, along with a slightly modified $L_3$, produced both acceptable pilot input responses and acceptable levels of control surface activity. The newly found $K_3$ also satisfied the desired eigenstructure of $[A_3 + BK_3]$. Pilot input

**Table 6 $K$ matrix elements**

| $k_{ij}$ | FC3 | FC6 |
|---|---|---|
| $k_{11}$ | 1.8318 E − 3 | 1.2043 E − 3 |
| $k_{12}$ | 2.3991 E − 5 | 3.5302 E − 6 |
| $k_{13}$ | −3.7022 E − 1 | −4.9738 E − 1 |
| $k_{14}$ | 2.0127 E − 1 | 2.3281 E0 |
| $k_{15}$ | 5.7078 E − 2 | −3.3838 E − 2 |
| $k_{16}$ | −5.8449 E − 1 | 2.3930 E − 1 |
| $k_{17}$ | 0 | 0 |
| $k_{18}$ | −2.2562 E − 3 | −1.1521 E − 1 |
| $k_{19}$ | −1.2191 E − 1 | −3.9166 E − 2 |
| $k_{1,10}$ | 1.3696 E − 2 | −1.7849 E − 1 |
| $k_{1,11}$ | 9.8792 E − 2 | −3.2314 E − 1 |
| $k_{1,12}$ | −6.5414 E − 2 | 7.7788 E − 1 |
| $k_{1,13}$ | −4.9203 E − 2 | −5.6376 E − 3 |
| $k_{1,14}$ | 1.9756 E − 2 | 8.6686 E − 3 |
| $k_{1,15}$ | 4.2341 E − 1 | −6.8332 E − 2 |
| $k_{21}$ | −1.1993 E − 3 | 1.4922 E − 4 |
| $k_{22}$ | −1.483 E − 5 | 1.6191 E − 6 |
| $k_{23}$ | −1.4327 E − 1 | 5.0179 E − 1 |
| $k_{24}$ | −3.1908 E − 1 | −1.8009 E0 |
| $k_{25}$ | −3.2513 E − 2 | −1.2139 E − 2 |
| $k_{26}$ | 3.6511 E − 1 | 6.5116 E − 2 |
| $k_{27}$ | 0 | 0 |
| $k_{28}$ | 3.7315 E − 2 | 3.4695 E − 2 |
| $k_{29}$ | 1.4484 E − 2 | −6.5762 E − 3 |
| $k_{2,10}$ | −1.7055 E − 3 | 6.1213 E − 2 |
| $k_{2,11}$ | 1.3834 E − 1 | 1.4678 E − 1 |
| $k_{2,12}$ | 6.9819 E − 3 | −1.7869 E − 1 |
| $k_{2,13}$ | 9.0369 E − 2 | 6.4177 E − 2 |
| $k_{2,14}$ | −6.1725 E − 2 | −4.3204 E − 2 |
| $k_{2,15}$ | −1.1903 E − 1 | 2.7929 E − 1 |
| $k_{31}$ | −4.1857 E − 3 | 5.5101 E − 3 |
| $k_{32}$ | −6.9868 E − 5 | −4.3752 E − 6 |
| $k_{33}$ | −9.4764 E − 1 | 9.1435 E − 1 |
| $k_{34}$ | 2.2050 E − 1 | −2.0149 E0 |
| $k_{35}$ | −2.6881 E − 1 | 6.6593 E − 1 |
| $k_{36}$ | 1.5745 E0 | −4.7519 E0 |
| $k_{37}$ | 0 | 0 |
| $k_{38}$ | −2.8257 E − 1 | 8.4993 E − 1 |
| $k_{39}$ | −5.8304 E − 1 | −1.7031 E − 1 |
| $k_{3,10}$ | −3.4420 E − 1 | 6.5872 E − 1 |
| $k_{3,11}$ | 2.3198 E − 1 | 3.3096 E0 |
| $k_{3,12}$ | 1.6945 E0 | −2.9226 E0 |
| $k_{3,13}$ | −7.2046 E − 2 | −1.5902 E − 1 |
| $k_{3,14}$ | 8.4586 E − 2 | −2.9615 E − 1 |
| $k_{3,15}$ | −1.2471 E0 | −1.2051 E0 |
| $k_{41}$ | 4.2557 E − 3 | 8.5448 E − 3 |
| $k_{42}$ | 4.6297 E − 5 | 1.5320 E − 5 |
| $k_{43}$ | −8.9088 E − 1 | 2.5780 E0 |
| $k_{44}$ | 7.3577 E − 1 | −1.4721 E0 |
| $k_{45}$ | −1.1896 E − 2 | 1.4309 E − 3 |
| $k_{46}$ | −1.1237 E0 | −3.5777 E − 2 |
| $k_{47}$ | 0 | 0 |
| $k_{48}$ | 2.3074 E − 2 | −4.7939 E − 3 |
| $k_{49}$ | −8.5158 E − 1 | −1.4595 E − 1 |
| $k_{4,10}$ | −2.4345 E − 1 | −2.3028 E − 1 |
| $k_{4,11}$ | 6.9392 E − 1 | 1.8835 E − 1 |
| $k_{4,12}$ | 6.5067 E − 1 | 5.8056 E − 1 |
| $k_{4,13}$ | 7.2557 E − 2 | 8.3421 E − 2 |
| $k_{4,14}$ | −3.6831 E − 2 | −4.2276 E − 2 |
| $k_{4,15}$ | −1.3184 E − 1 | 2.1986 E − 1 |
| $k_{51}$ | 7.7201 E − 4 | −4.1058 E − 4 |
| $k_{52}$ | 1.0058 E − 5 | 7.6467 E − 7 |
| $k_{53}$ | −2.0336 E − 1 | −8.5046 E − 1 |
| $k_{54}$ | 4.5271 E − 1 | 8.9537 E − 1 |
| $k_{55}$ | 1.0456 E − 2 | −4.6597 E − 2 |
| $k_{56}$ | −2.5931 E − 1 | 3.3938 E − 1 |
| $k_{57}$ | 0 | 0 |
| $k_{58}$ | 4.0275 E − 4 | −8.9257 E − 2 |
| $k_{59}$ | −8.6797 E − 3 | −4.6243 E − 2 |
| $k_{5,10}$ | −4.0726 E − 3 | −9.2840 E − 2 |
| $k_{5,11}$ | 3.1287 E − 2 | −3.6111 E − 1 |
| $k_{5,12}$ | 1.5898 E − 2 | 4.1073 E − 1 |
| $k_{5,13}$ | 9.6257 E − 4 | 4.9318 E − 2 |
| $k_{5,14}$ | 4.0689 E − 4 | 2.1704 E − 2 |
| $k_{5,15}$ | 4.4526 E − 1 | 7.4055 E − 1 |

pulses for $\delta_{AC}(t)$ and $\delta_{RC}(t)$ were also applied in FC1 and in FC3 with the final $L_3$ and $K_3$ designs, and the responses to these inputs were also found to match to a satisfactory degree.

For FC6 a similar design procedure for $L_6$ and $K_6$ was followed and results similar to those described above for FC3 were achieved. The final values for the elements of $L_3$ and $L_6$ are given in Table 5, and those for $K_3$ and $K_6$ are in Table 6.

## Results and Discussion

The zero input responses for FC3 and FC6 for the configuration shown in Fig. 2 and with the $K_3$ and $K_6$ matrix elements given in Table 6 are shown in Fig. 4. In each case here the initial state is zero, except for $x_9(0) = \dot{\theta}(0)$, whose value is 1 deg/s. These responses may be compared with those shown in Fig. 1. The decoupling of the lateral motions of the airframe from the longitudinal motions by the feedback matrix $K$ in FC3 and FC6 is pronounced. The $\theta(t)$ responses in FC3 and FC6 are qualitatively similar to the "ideal," that of FC1, shown in Fig. 1.

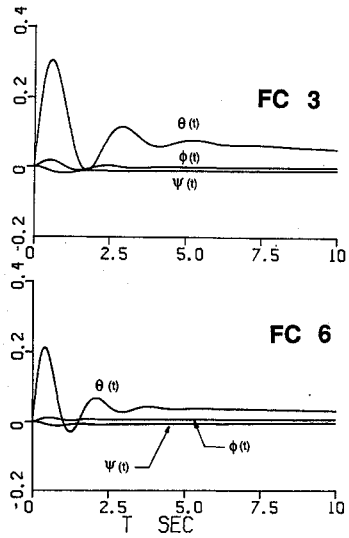


**Fig. 4 ZIR to $\dot{\theta}_o = 1$ deg/s for final $K_3$ and $K_6$ designs. Deflections given in degrees.**

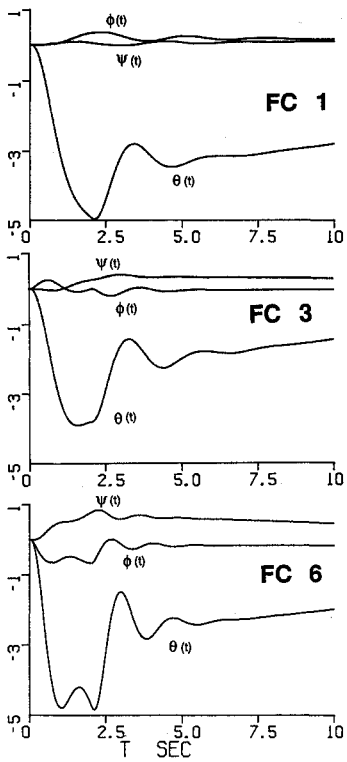


**Fig. 5 Responses to 1 deg stabilizer command, pulse duration 2 s. Deflections given in degrees.**

Comparisons of zero input responses for FC3 and FC6 to the corresponding "ideal" response of FC1 were also made for initial conditions of $x_8(0) = \dot{\phi}(0) = 1$ deg/s and for $x_{10}(0) = \dot{\psi}(0) = 1$ deg/s. The results of those tests (not shown here) revealed that the zero input responses for FC3 and FC6, using the $K$ matrix feedback, were qualitatively similar to the corresponding responses of FC1.

Pilot input tests, in the configuration shown in Fig. 3, were conducted using a commanded stabilizer pulse of 2 s duration and having an amplitude of 1 deg, as described above. Fig. 5 shows the results for FC1, FC3, and FC6 in response to this stabilizer command. We note that the decoupling is very effective in FC3 and acceptable in FC6. The $\theta(t)$ responses are qualitatively similar between FC1 and FC3, and nearly so for FC6. It is of interest to note the control surface deflections that are required to produce these decoupled responses. These are shown in Fig. 6 for FC3 and in Fig. 7 for FC6. The limits on

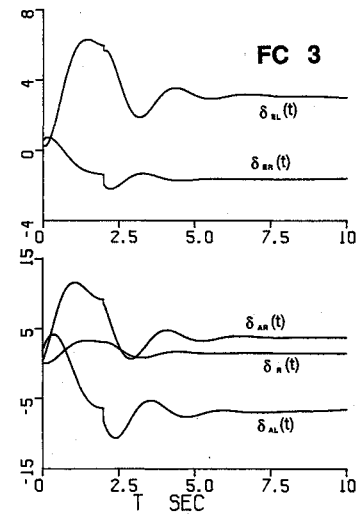


**Fig. 6 Control surface deflections in response to 1 deg stabilizer command pulse, FC3. Deflections given in degrees.**

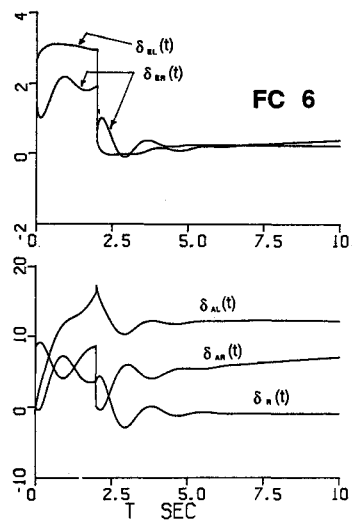


**Fig. 7 Control surface deflections in response to 1 deg stabilizer command pulse, FC6. Deflections given in degrees.**

deflection rates for the control surfaces given in Table 2 were not incorporated in the simulation for these tests, but they are exceeded during these small signal tests only momentarily ($t \sim 2$ s).

Comparisons of pilot input responses for pulses of aileron command and rudder command were also made. The results of those tests, not shown here, were similar to those for the stabilizer command in that the responses for FC3 and FC6 were qualitatively similar to those of FC1.

## Conclusions

The work reported here shows that the eigenstructure design method can be combined with an optimization procedure to yield results that are useful in the design of a nondynamic command and stability augmentation system for the oblique wing research airplane. This is demonstrated by calculating the two control law matrices that define the command and stability augmentation system for flight conditions in which the wing skew angle is large, and showing (by simulation) that transient responses from initial conditions and from pilot inputs approximate the corresponding transient responses obtained when the wing skew angle is zero. The deflections and rates of deflection of the five primary control surfaces are reasonable during these manuevers. The comprehensive air data and inertial instrumentation in this airplane contributes significantly to the feasibility of the eigenstructure design method.

## Appendix A

The elements of the $A_{AF}$ and $B_{AF}$ matrices in Eq. (3) for the three flight conditions described in Table 1 are listed below. In this listing $a_{ij}$ is the element in the $i$th row and the $j$th column of $A_{AF}$, and $b_{ij}$ is the element in the $i$th row and the $j$th column of $B_{AF}$. The elements having zero value are omitted.

## Appendix B: Optimization Method

The Davidon, Fletcher, and Powell algorithm, based on conjugate gradient methods, is used here.[9] Because $C_i$ is a quadratic form, its gradient is easily calculated:

$$\frac{\partial C_i}{\partial \gamma_i} = 2\alpha_i(\gamma_i - \lambda_{id}) \tag{B1a}$$

$$\frac{\partial C_i}{\partial V_i} = 2[Q_i(V_i - V_{id})] \tag{B1b}$$

$$\frac{\partial C_i}{\partial w_i} = 2\beta_i w_i \tag{B1c}$$

We note that whereas $C_i$ is real-valued, the quantities in Eq. (B1) are complex-valued because $\gamma_i$, $V_i$, and $w_i$ are complex-valued. We wish to calculate the small variation in $C_i$, which is induced by small variations in $\gamma_i$, $V_i$ and $w_i$ that are

$$d\gamma_i = d\gamma_{iR} + j\, d\gamma_{iI} \tag{B2a}$$

$$dV_i = dV_{iR} + j\, dV_{iI} \tag{B2b}$$

$$dw_i = dw_{iR} + j\, dw_{iI} \tag{B2c}$$

**Table A1 Elements of $A_{AF}$ and $B_{AF}$**

| $a_{ij}$ | FC1 | FC3 | FC6 | $a_{ij}$ | FC1 | FC3 | FC6 |
|---|---|---|---|---|---|---|---|
| $a_{11}$ | −7.53131 E − 3 | −2.4068 E − 2 | −1.5288 E − 2 | $a_{93}$ | −6.29754 E0 | −1.7104 E + 1 | −2.2103 E + 1 |
| $a_{12}$ | 1.00081 E − 5 | −3.1396 E − 5 | 1.8476 E − 4 | $a_{94}$ | 0 | 1.2468 E − 1 | 3.8057 E0 |
| $a_{13}$ | 1.91377 E + 1 | 5.0943 E − 1 | −1.9503 E + 1 | $a_{98}$ | 1.48542 E − 3 | 1.4226 E − 1 | 8.8938 E − 2 |
| $a_{14}$ | 0 | 1.2694 E + 1 | 1.3179 E + 1 | $a_{99}$ | −7.12991 E − 1 | −1.2694 E0 | −1.2187 E0 |
| $a_{15}$ | 0 | −2.7833 E − 1 | −2.9294 E − 1 | $a_{9,10}$ | 1.0012 E − 1 | 1.9855 E − 1 | 2.4095 E − 1 |
| $a_{16}$ | −3.21277 E + 1 | −3.2112 E + 1 | −3.2080 E + 1 | $a_{10,1}$ | 0 | −7.1016 E − 4 | −7.8374 E − 4 |
| $a_{18}$ | 0 | 1.3543 E − 2 | 1.3999 E − 2 | $a_{10,2}$ | 0 | −1.0531 E − 6 | −3.7871 E − 6 |
| $a_{19}$ | 0 | −1.3767 E − 3 | −5.5942 E − 4 | $a_{10,3}$ | 0 | −2.0223 E0 | −7.5461 E0 |
| $a_{1,10}$ | 0 | −6.8769 E − 2 | −6.9607 E − 2 | $a_{10,4}$ | 6.14001 E0 | 1.2953 E + 1 | 1.8778 E + 1 |
| $a_{23}$ | −6.34401 E + 2 | −9.332 E + 2 | −1.3927 E + 3 | $a_{10,8}$ | −1.2752 E − 1 | 3.5635 E − 2 | 7.0071 E − 2 |
| $a_{25}$ | 0 | 8.0886 E0 | 1.2718 E + 1 | $a_{10,9}$ | −9.45255 E − 2 | −5.0017 E − 3 | −6.8218 E − 2 |
| $a_{26}$ | 6.34401 E + 2 | 9.3320 E + 2 | 1.3927 E + 3 | $a_{10,10}$ | −6.67316 E − 1 | −9.2424 E − 1 | −9.6575 E − 1 |
| $a_{31}$ | −1.80473 E − 4 | −7.3947 E − 5 | −2.1382 E − 5 | $b_{11}$ | 1.73445 E0 | −1.8696 E0 | −3.5782 E0 |
| $a_{32}$ | 1.60142 E − 6 | 1.1175 E − 6 | 8.7575 E − 7 | $b_{12}$ | 1.73445 E0 | −2.1894 E0 | −3.6661 E0 |
| $a_{33}$ | −9.86537 E − 1 | −8.0388 E − 1 | −5.6285 E − 1 | $b_{13}$ | −7.70872 E − 1 | −3.2780 E − 1 | 5.0819 E − 1 |
| $a_{34}$ | 0 | 8.0292 E − 2 | 6.6539 E − 2 | $b_{14}$ | −7.70872 E − 1 | −1.3390 E0 | −1.4238 E0 |
| $a_{38}$ | 0 | 8.1353 E − 3 | 8.8719 E − 3 | $b_{15}$ | 0 | 4.4507 E0 | 6.5081 E0 |
| $a_{39}$ | 9.90119 E − 1 | 9.9209 E − 1 | 9.9509 E − 1 | $b_{31}$ | −8.87653 E − 2 | −1.1207 E − 1 | −7.2055 E − 2 |
| $a_{3,10}$ | 0 | −7.4879 E − 5 | 1.6842 E − 5 | $b_{32}$ | −8.87653 E − 2 | −1.1207 E − 1 | −7.2055 E − 2 |
| $a_{41}$ | 0 | 1.0635 E − 5 | 6.2741 E − 6 | $b_{33}$ | −4.11926 E − 2 | −1.5954 E − 2 | −1.5946 E − 3 |
| $a_{42}$ | 0 | 4.0219 E − 8 | 3.9743 E − 8 | $b_{34}$ | −4.11926 E − 2 | −2.1963 E − 2 | −1.1721 E − 2 |
| $a_{43}$ | 0 | −9.1789 E − 2 | −7.0535 E − 2 | $b_{41}$ | −1.19803 E − 2 | −1.9770 E − 2 | −3.4778 E − 3 |
| $a_{44}$ | −2.38641 E − 1 | −3.4593 E − 1 | −4.2091 E − 1 | $b_{42}$ | 1.19803 E − 2 | 1.9733 E − 2 | 3.4302 E − 3 |
| $a_{45}$ | 5.06409 E − 2 | 3.4381 E − 2 | 2.3013 E − 2 | $b_{43}$ | 0 | 3.4572 E − 5 | −4.9809 E − 3 |
| $a_{46}$ | 0 | −2.9849 E − 4 | −2.1052 E − 4 | $b_{44}$ | 0 | −8.2215 E − 4 | 6.7823 E − 4 |
| $a_{48}$ | 6.45849 E − 3 | 3.8537 E − 2 | 4.0855 E − 2 | $b_{45}$ | 5.38700 E − 2 | 5.7448 E − 2 | 2.0229 E − 2 |
| $a_{49}$ | 0 | 1.7006 E − 4 | 4.3946 E − 5 | $b_{81}$ | 7.96795 E0 | 1.9889 E + 1 | 4.4873 E + 1 |
| $a_{4,10}$ | −9.991114 E − 1 | −9.9070 E − 1 | −9.9365 E − 1 | $b_{82}$ | −7.96795 E0 | −3.3660 E + 1 | −5.9815 E + 1 |
| $a_{58}$ | 1.0000 E0 | 1.0000 E0 | 1.0000 E0 | $b_{83}$ | 1.91835 E + 1 | 1.4438 E + 1 | 3.9130 E0 |
| $a_{69}$ | 1.0000 E0 | 1.0000 E0 | 1.0000 E0 | $b_{84}$ | −1.91835 E + 1 | −1.0436 E + 1 | −6.8594 E0 |
| $a_{7,10}$ | 1.0000 E0 | 1.0000 E0 | 1.0000 E0 | $b_{85}$ | 6.08828 E0 | 1.8859 E + 1 | 1.4086 E + 1 |
| $a_{81}$ | 0 | −1.9511 E − 3 | 4.1348 E − 3 | $b_{91}$ | −6.05267 E0 | −1.2387 E + 1 | −1.3289 E + 1 |
| $a_{82}$ | 0 | 4.4807 E − 5 | 5.4499 E − 5 | $b_{92}$ | −6.50267 E0 | −1.4442 E + 1 | −1.6529 E + 1 |
| $a_{83}$ | 0 | 1.3318 E + 1 | 4.4889 E + 1 | $b_{93}$ | −1.22131 E − 1 | −1.2473 E0 | −4.6578 E − 1 |
| $a_{84}$ | −2.43879 E + 1 | −8.4826 E + 1 | −1.9057 E + 2 | $b_{94}$ | −1.22131 E − 1 | 9.2012 E − 1 | 1.4796 E0 |
| $a_{88}$ | −5.86251 E0 | −2.4565 E0 | −1.7391 E0 | $b_{95}$ | 0 | 7.4850 E − 1 | 4.6469 E − 1 |
| $a_{89}$ | −3.38595 E − 2 | 1.4708 E0 | 3.0771 E − 1 | $b_{10,1}$ | 1.0751 E0 | 2.8904 E0 | 2.5420 E0 |
| $a_{8,10}$ | 8.37616 E − 1 | 2.3459 E0 | 2.6033 E0 | $b_{10,2}$ | −1.0751 E0 | −3.2906 E0 | −2.9729 E0 |
| $a_{91}$ | −2.95692 E − 4 | −7.9564 E − 4 | 2.1731 E − 3 | $b_{10,3}$ | 5.8548 E − 1 | 4.6101 E − 1 | 3.8913 E − 2 |
| $a_{92}$ | −6.07674 E − 7 | −1.2731 E − 5 | 6.0607 E − 6 | $b_{10,4}$ | −5.8548 E − 1 | −2.9492 E − 1 | −5.6054 E − 1 |
| | | | | $b_{10,5}$ | −4.30492 E0 | −7.1025 E0 | −3.6587 E0 |

Now, we have for $\partial C_i/\partial \gamma_i$

$$\frac{\partial C_i}{\partial \gamma_i} = \frac{\partial C_i}{\partial \gamma i_R} + j\,\frac{\partial C_i}{\partial \gamma_{iI}} \tag{B3}$$

and there are like expressions for $\partial C_i/\partial V_i$ and $\partial C_i/\partial w_i$.

Consequently, the variation in $C_i$ is (to a first-order approximation)

$$\begin{aligned} \mathrm{d}C_i = {} & \frac{\partial C_i}{\partial \gamma_{iR}}\,\mathrm{d}\gamma_{iR} + \frac{\partial C_i}{\partial V_{iR}}\,\mathrm{d}V_{iR} + \frac{\partial C_i}{\partial w_{iR}}\,\mathrm{d}w_{iR} \\ & + \frac{\partial C_i}{\partial \gamma_{iI}}\,\mathrm{d}\gamma_{iI} + \frac{\partial C_i}{\partial V_{iI}}\,\mathrm{d}V_{iI} + \frac{\partial C_i}{\partial w_{iI}}\,\mathrm{d}w_{iI} \end{aligned} \tag{B4}$$

Now, $\gamma_i$, $V_i$, and $w_i$ must satisfy the constraint Eq. (18). Therefore, the variations $\mathrm{d}\gamma_i$, $\mathrm{d}V_i$, and $\mathrm{d}w_i$ must be such that

$$\mathrm{d}[A - \gamma_i I)V_i + Bw_i] = 0 \tag{B5}$$

Thus, we have

$$\begin{aligned} & (A - \gamma_i I)(\mathrm{d}V_{iR} + j\,\mathrm{d}V_{iI}) + B(\mathrm{d}w_{iR} + j\,\mathrm{d}w_{iI}) \\ & - (\mathrm{d}\gamma_{iR} + j\,\mathrm{d}\gamma_{iI})V_i = 0 \end{aligned} \tag{B6}$$

Eq. (B6) is combined with (B2) to eliminate $\mathrm{d}V_i$ from the variation given in (B4). That variation can then be expressed as a constrained variation involving only $\mathrm{d}\gamma_i$ and $\mathrm{d}w_i$:

$$\mathrm{d}C_i^c = \frac{\partial C_i^c}{\partial \gamma_{iR}}\,\mathrm{d}\gamma_{iR} + \frac{\partial C_i^c}{\partial w_{iR}}\,\mathrm{d}w_{iR} + \frac{\partial C_i^c}{\partial \gamma_{iI}}\,\mathrm{d}\gamma_{iI} + \frac{\partial C_i^c}{\partial w_{iI}}\,\mathrm{d}w_{iI} \tag{B7}$$

where

$$\frac{\partial C_i^c}{\partial \gamma_i} = 2\alpha_i(\gamma_i - \lambda_{id}) + 2[Q_i(V_i - V_{id})]^T\overline{[A - \gamma_i I]^{-1}V_i} \tag{B8a}$$

$$\frac{\partial C_i^c}{\partial w_i} = 2\beta_i w_i^T - 2[Q_i(V_i - V_{id})]^T\overline{[(A - \gamma_i I)^{-1}B]} \tag{B8b}$$

where $V_i$ is expressed in terms of $\gamma_i$ and $w_i$ from Eq. (20)

$$V_i = -(A - \gamma_i I)^{-1}Bw_i \tag{B9}$$

and $(A - \gamma_i I)^{-1}$ is conveniently calculated as

$$(A - \gamma_i I)^{-1} = P[\Lambda - \gamma_i I]^{-1}P^{-1} \tag{B10}$$

Here, $P$ is an equivalence transformation that diagonalizes $A$ and $\Lambda = \mathrm{diag}[\lambda_i]$ where $\lambda_i$ is the $i$th eigenvalue of $A$. We assume that $\gamma_i$ in (B8) is not an eigenvalue of $A$. Thus (B8) substituted into (B7) gives the form

$$\frac{\partial C_i^c}{\partial \gamma_i} = f(\gamma_i, w_i, \alpha_i, Q_i) \tag{B11a}$$

$$\frac{\partial C_i^c}{\partial w_i} = g(\gamma_i, w_i, \beta_i, Q_i) \tag{B11b}$$

The optimization algorithm follows this schedule:

1) The program must be initialized with $\gamma_{io}$, $w_{io}$, and a metric matrix $H_o = I_{(m+1)}$. $H$ is described below. A sequence $\{\gamma_i(k), w_i(k)\}$ is then calculated recursively. At the end of step $(k-1)$ values for $\gamma_i(k)$, $w_i(k)$, and $H(k)$ are available. The $k$th step then follows.

2) Compute the constrained gradient $\nabla C_i^c(k) = [f,g]^T$ [see (B7)–(B11) above].

3) Compute the search direction $S_k = -H(k)\nabla C_i^c(k)$. $S_k$ is $(m+1) \times 1$ if $\gamma_i$ is real, and $2(m+1) \times 1$ if $\gamma_i$ is complex.

4) $\gamma_i$ and $w_i$ are incremented from $\gamma_i(k)$ and $w_i(k)$ in the direction given by $S_k$, until a minimum $C_i^c(\gamma_i, w_i)$ is found. This gives $\gamma_i(k+1)$, $w_i(k+1)$, and $C_i^c(k+1)$. $H(k+1)$ is then calculated as

$$H(k+1) = H(k) + (p_k p_k^T/p_k^T y_k) - (H(k)y_k y_k^T H(k)/y_k^T H(k)y_k) \tag{B12}$$

where

$$\begin{aligned} y_k &= [\nabla C_i^c(k+1)]^T - [\nabla C_i^c(k)]^T \\ p_k &= (\gamma_i/w_i)_{k+1} - (\gamma_i/w_{ik})_k \end{aligned} \tag{B13}$$

5) Test for stop, else continue the iteration with step 3, replacing $k$ by $k+1$.

6) The program performs $n$ iterations, stops and displays the norm of the gradient $C_i^c(n)$ and $\gamma_i(n)$. The operator decides whether to continue the descent or to terminate the sequence.

7) These steps are repeated for $i = 1,2...15$. The initial value $\gamma_{io}$ is taken to be $\lambda_{id}$; $w_{io}$ is then calculated from Eq. (13) as

$$w_{io} = -(B^T B)^{-1}B^T[A - \lambda_{id}I]V_{id} \tag{B14}$$

It is important that the initial guesses be good ones since in this 15th-order system there may be more than one local minimum of $C_i^c$.

## References


[1]Jones, R. T., "Flying-Wing SST for the Pacific," *Aerospace America*, Vol. 24, Nov. 1986, pp. 32–33.

[2]Curry, R. E. and Sim, A. G., "Unique Flight Characteristics of the AD-1 Oblique Wing Research Airplane," *Journal of Aircraft*, Vol. 20, June 1983, pp. 564–68.

[3]Alag, G. S., Kempel, R. W., and Pahle, J. W., "Decoupling Control Synthesis for an Oblique-Wing Aircraft," *Proceedings of the American Control Conference*, American Automatic Control Council, Seattle, WA, June 1968, p. 472.

[4]"Oblique Wing Control Design," NASA Ames Research Center/Dryden Research Center, PR OP-1127, Exhibit A, Nov. 1985.

[5]Porter, B. and D'Azzo, J. J., "Closed Loop Eigenstructure Assignment by State Feedback in Multivariable Linear Systems," *International Journal of Control*, Vol. 27, March 1978, pp. 287–292.

[6]Cunningham, T. B., "Eigenspace Selection Procedures for Closed Loop Response Shaping with Modal Control," *Proceedings of the 1980 IEEE Control and Decision Conference*, IEEE, New York, pp. 178–186.

[7]Brogan, W. L., "Modern Control Theory," 2nd ed., Prentice-Hall, New York, 1985.

[8]Wonham, W. M., "Linear Multivariable Control: A Geometric Approach," 2nd ed., Springer-Verlag, New York, 1979.

[9]Pearson, J. D., "Variable Metric Methods of Minimisation," *Computer Journal*, Vol. 12, 1969, pp. 171–178.